1998 International Computer Symposium
Workshop on Image Processing and Character Recognition
December 17-19, 1998, N.C.K.U., Tainan, Taiwan, R.O.C.

MEASUREMENT OF INTRA-KNEE JOINT SPACING OF THE FEMUR AND TIBIA USING X-RAY FILM IMAGES

Timothy L.J. Ferris

School of Physics and Electronic Systems Engineering,
University of South Australia, Mawson Lakes, Australia
Email: timothy.ferris@unisa.edu.au

ABSTRACT

This paper describes a method to determine the alignment of the femur-tibia spacing using a standard X-ray study of the human knee, front view of the leg taken in the lying position, where there is no weight load on the knee. The method involves analysis of an outline image of the bones around and including the knee joint, requiring sufficient length of both femur and tibia to enable a meaningful estimate of the bone orientation. This length is normally provided in the X-ray film exposure. The method estimates the bone orientation based on finding a centreline between two straight line approximations to the bone edges, found using a threshold criterion on the Mean Square Error of the bone edge and the estimate. The normal to this line is found to provide a definition of the width of the joint, and a plot of the distance between the femur and tibia is produced over the full width of the joint. The method automatically distinguishes the tibia and fibula in the lower leg region.

INTRODUCTION

The knee joint involves four bones; the femur, which extends from hip to knee; the tibia, the main lower leg bone; the patella, which assists the mechanical function of the knee; and the fibula, which assists foot control. The knee joint also includes soft tissues, menisci, ligaments, tendons and muscles. Some of these soft elements are located between the femur and the tibia, filling the space between the bones. Some diseases or injuries of the knee which are only partially indicated, if at all, by changes in the bones but are further characterised by a change in the spacing of these bones. Consequently a means to measure the distance between the femur and the tibia would appear to be helpful to an orthopaedic surgeon in the task of diagnosing arthritis. Since the ends of the femur and tibia are curved in three dimensions a definition of a measure is required in order to produce a useful measurement result.

X-RAY IMAGE FEATURES

This study has used X-ray film images of the leg of a subject lying on their back, exposed from the front. This image is one of the standard knee study set, produced when the subject's leg is comfortably resting with no applied weight load. We digitised the X-ray film with an office quality scanner, producing a 650 x 849 x 256 grey level TIFF image, scanned with a resolution of 86 pixels per inch.

This process requires an edge image with single pixel wide continuous edge, called the edge image. The edge image requires subjection of the original image to an edge detection process, which continues to be the subject of research, with imperfect results reported in Ferris and Stewein [1]. The process used in this study was part of the preliminary studies in the edge detection work. The image was first subjected to a Sobel Compass edge detection operator, followed by a threshold operation [2]. Various artefacts, originating in the scanning process and from uneven exposure and drying stains on the film were found. In order to overcome the effect of the artefacts the scanned image was pre-filtered using the LUM filter of Boncelet and Hardie [3,4], followed by the Sobel Compass operator and a threshold pass. The LUM filter is a statistical filter, operating on the rank-order of pixel colours in a square segment centred on the pixel of interest. The effect of the LUM filter is to apply simultaneous sharpening and softening to an image, so that artefacts are removed by the softening and significant objects are detected by sharpening. Three parameters are fed to the LUM filter, the dimensions of the segment, a sharpening factor and a softening factor. We found, empirically, that the combination, 7×7 LUM filter, with softening and sharpening factors both 2, followed by Sobel Compass operator with threshold between 25 and 30, produced reasonably artefact free edge images, with some 'thick' edges. We manually edited the resultant imperfect edge image with an image editor to obtain single pixel wide continuous edges. Figure 1 shows our edited test image, with centrelines indicated.

DEFINITIONS

We define several terms used repeated through this paper:

Backtracking. Backtracking is tracing a bone edge back to the image edge from the first point in the image where the edge is detected and recognised as an edge. Backtracking is illustrated in figure 2.

Distance Measure. This measure is based on a reference point added to the original image and rotated with it. The Euclidean distance between rotated reference point and

the centreline intersection point is the Distance Measure.

Horizontal image. The image of figure 1 is oriented such that both edges of the tibia and femur intersect with the left and right vertical margins of the image. This orientation is called 'horizontal'.

Rotation. Rotation of the image is relative to the orientation of figure 1, the primary image in all experimental work reported in this paper, with the centre of rotation located at the image centre.

Femur-Tibia Spacing. The femur-tibia spacing is the graph of the dimension between the femur and tibia.

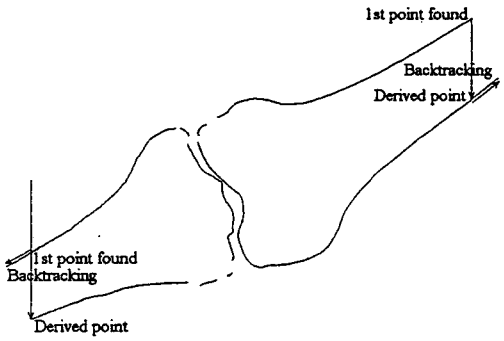

Figure 1. Edge image of the knee front view X-ray image, with femur and tibia straight-line edge approximations, centrelines and intersection angle indicated. This image is in the orientation called 'horizontal'. This image was rotated about the image centre point by angles of -25° to +25° in steps of 5° for test purposes.

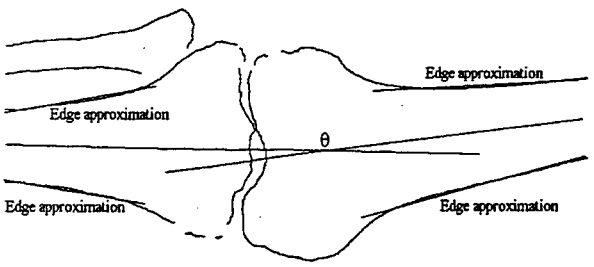

Figure 2. The edge starting points found using the simple method and backtracking, for an image where the femur and tibia straddle a corner.

RELEVANT BONE FEATURES

Standard knee study images place the knee approximately at the centre of the image and usually position the femur and tibia approximately perpendicular to the edges. Normally the film size is chosen to show about 5 cm to 10 cm of the 'straight' shaft segment of each of the femur and tibia. Immediately around the joint both the femur and tibia are considerably thickened. This part of each bone is unusable for determination of the bone centreline. Both the femur and tibia in the region far from the knee joint have slowly curving edges which can be approximated to straight lines using a parametric definition of sufficiently close approximation to a straight line. The femur, at the top of the leg is a single bone, and so there are 2 edges, which intersect with image boundary. The tibia is in the lower part of the leg, adjacent to the fibula, so there are four bone edges to intersect with image boundary.

METHOD

We defined the bone spacing dimension sought as the graph of the spacing across the joint, with both axes calibrated in millimetres. This presentation of the result preserves the spatial characteristics of the dimension function, avoiding the problem of attempting to reduce the geometric quantity to a single number, which would not preserve the same amount of geometric information. The need for a function of space to be sought results from the possibility that with various deformities of the knee different parts of the knee may receive different amounts of dimensional distortion, and the fact that the geometry of the ends of the femur and tibia are complex, and bear no clear geometric relation. The femoral condyles are large, sharply curved forms with a clear, rounded depression between them. The matching part of the tibia is curved, with a much flatter form, and at the centre, between the seating positions of the femoral condyles, is a sharp projection. The shapes of these two portions of the bones do not permit a simple geometric description of the shapes to be presented, and so preclude derivation of a spacing function where derivation of parameters in the formula may be used as the basis of a measurement. In addition, if any such approach were found, the measure would be desensitised to spacing distortions affecting part of the joint, or involving a wedge shape change, increasing spacing on one side and decreasing spacing on the other side. Presentation of a plot of the spacing across the whole joint maintains the presentation of this spatial information.

An algorithm capable of finding the spacing dimension function under various rotations, translations and reflections of the bone images relative to the image boundary was required. The possibility of rotations, translations and reflections simulates both left and right legs and the arbitrary orientation of the exposure on the film. It is desirable to produce a visual check image including the bone centre-lines, and a processing failure error message. This enables the user to quickly determine if the automated image recognition rules implemented, described below, have produced reasonable results. The algorithm implemented assumes the edge image contains only single pixel wide, continuous edges with bone edge ends at the image edge. Our algorithm assumes 'horizontal' image presentation, as in figure 1. Image rotation is allowed so long as there remains a vertical cross section through which both edges of each major

bone pass. Should this condition fail the image is 'vertical' and must be rotated 90° to produce a 'horizontal' image.

The algorithm has four stages:

1. Find the femur and tibia edges;
2. Calculate the femur and tibia centrelines;
3. Calculate the centrelines intersection point;
4. Find the line that bisects the intersection point of the two centrelines, the Bisecting Line, BL.
5. Find the normal to BL.
6. Translate the normal to BL across the joint to find the outer limits of the region for which the normal touches both femur and tibia at some position along its length.
7. Find the distance along the normal to BL between the femur and the tibia at intervals of one pixel for all points along BL inside the range determined in part 6.
8. Create a plot of the result of step 7.

The algorithm requires one user-specified parameter, the Mean Square Error, MSE, allowed for the straight line fitting of the bone edges. The remainder of the algorithm is fixed.

The bone edge approximation is found and mathematically described in two phases:

1. Find edge starting points;
2. Find the mathematical description of the edge.

The edge starting points may be found using a simple image search. To find one set of edges start the search at the left of the image, checking each vertical line of pixels until one is found with two non-neighbour edge pixels. Similarly, the image is to be searched from the right until the first vertical line containing two non-neighbour edge pixels is found. Continue each search until a vertical line containing four non-neighbour edge pixels is found. The side with only two edge pixels found is the femur side of the knee, and that with four is the tibia side of the joint. If the image is rotated from horizontal, or straddling a corner, the starting points found may not be the real first points of the bone edges, see figure 2. Backtracking is used to ensure the real first point of the bone edge is found. When four non-neighbour edge pixels are detected backtracking is used to ensure that they terminate at an edge of the image. If not the four points do not define edges of the tibia and fibula and the search must be continued. The result of backtracking is a better bone edge approximation, based on a longer 'straight' segment of the edge.

It is assumed that the bone edges in the central sections of the femur and tibia can each be approximated by a straight line and that the edge starting points found are in the region where this assumption is reasonable. A line of best fit is sought, building along the edges from the start points towards the image centre. A line fitting, using the least square method, is done on the first 5 edge pixels. If the image is rotated from horizontal, or straddling a corner, the starting points found may not be the real first points of the bone edges, see figure 2. Backtracking, meaning moving towards the nearest image edge, is used to ensure the real first point of the bone edge is found. Then, while the MSE of the fitted line is less than the user-specified threshold, more edge points are added to the approximation. This method maximises the length of the fitted line whilst maintaining the threshold MSE and so maximises the result accuracy. This method would fail only if the bone edge exhibited 'lumps', rather than the expected smooth curve. The Least Square Method is used to find the straight-line approximation of a sequence of edge points, so minimising the Total Square Error, *TSE*:

$$TSE = \min \sum_{m} ((a.x_i + b) - y_i)^2 \qquad (1)$$

Where x_i is the x-coordinate and y_i is the y-coordinate of the *i*th edge point evaluated along the real curve on the edge image, (x_i, y_i). $a.x_i+b$ determines the *y*-coordinate of the estimated approximation line that must be compared with the real *y*-coordinate at the same *x*-coordinate, x_i. *m* is the number of edge points included in the fitting process, and *a* and *b* are the parameters of the estimated approximation line. The fitting parameters *a* and *b* can be found using:

$$a = \frac{m\sum_{m} x_i y_i - \sum_{m} x_i \sum_{m} y_i}{m\sum_{m} x_i^2 - (\sum_{m} x_i)^2}$$

$$b = \frac{\sum_{m} y_i - a\sum_{m} x_i}{m} \qquad (2)$$

The MSE is used to test the fit quality. The total fit error is found using (1) and is related to MSE by:

$$MSE = \frac{TSE}{m} = \frac{\sum_{m} (y - y_i)^2}{m} \qquad (3)$$

The value of MSE required for a certain dimensional quality of fit is dependent on image resolution because it is expressed in [pixel^2]. This value can be transformed to a dimensioned quantity, free of image resolution constraints; ie transform from [pixel^2] to [mm^2].

To fit a line to a series of edge points in a bitmap one must trace a line through the image. The search routine finds the next point given the coordinates of the current and previous points using a 3×2 mask in which the next point must be located. The order of searching the neighbouring pixels for an edge point depends on the method chosen, figure 3 a,b. Both variants appear similar but the second is significantly superior to the first because it prevents

blind turns, as shown in figure 4. The second method was used here. This method is dependent on single pixel width and continuity of the edge being traced.

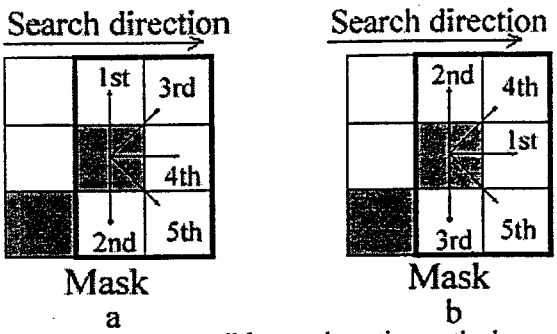

Figure 3. The two possible search routine methods.

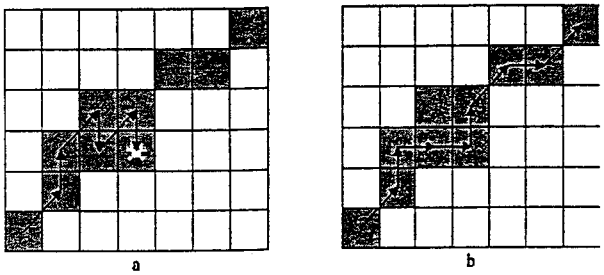

Figure 4. Effect of line following using both methods of figure 3.

After describing the bone edges, calculation of the centreline is easy. If we have two equations, $y_1 = a.x+b$ and $y_2 = c.x+d$; where $y_1 > y_2$ describing the bone edges the bone centreline is found:

$$y_m = \left(\frac{y_1 - y_2}{2}\right) + y_2 = \left(\frac{y_1 + y_2}{2}\right) \tag{4}$$

which simplifies to:

$$y_m = \left(\frac{a-b}{2}\right).x + \left(\frac{b+d}{2}\right) \tag{5}$$

Both centre lines can be found as: $y_{m1} = e.x+f$ and $y_{m2} = g.x+h$, and the x and y coordinates of their intersection, x_{cross} and y_{cross}, can be found:

$$x_{cross} = \left(\frac{f-h}{g-e}\right) \tag{6}$$

$$y_{cross} = e.x_{cross} + f = g.x_{cross} + h$$

Given the two centreline slopes, the slope of the line bisecting the angle of intersection of the two centrelines, BL, may be found:

$$h = -\left(\frac{1}{e} + \frac{1}{g}\right) \tag{7}$$

The normals to BL have slope:

$$k = -\frac{1}{h} = \frac{e.g}{e+g} \tag{8}$$

The normals to BL are then translated to determine the outer bounds of the region for which the normal intersects both the femur and tibia outline. The distance between the femur and the tibia is found, at one pixel intervals throughout the range of the knee joint, and the results are written to a graph of the dimensions.

EXPERIMENTS

Experiments were performed with knee X-ray images, like the bone outlines shown in figure 1. The images used were derived from a 6 year old male subject, and were digitised in a 849x650 256 grey level image with resolution of 0.295 mm per pixel in horizontally and vertically. As explained above an edge image was produced using a LUM filter followed by a Sobel compass edge detection operator and a threshold which was then manually edited to produce single pixel wide continuous edges. The algorithm for determination of the femur and tibia spacing dimension was then applied.

In a separate, but related study, of the measurement of the femur and tibia alignment, which uses the same bone centreline determination technique, in order to find the alignment angle and centreline intersection point five values for the allowed fitting error (0.5, 1, 2, 3 and 4 [pixel^2]), *MSE* in equation 3, and eleven angles of rotation of the image, -25° to 25° in 5° steps, were chosen. In each case the effect of finding the starting points with and without backtracking was tested. In each case the alignment angle and the centreline intersection point were recorded.

Clearly the bones described by the outline image maintain their relative alignment regardless of the image rotation, which only changes the bone alignment relative to the image boundary reference frame. The purpose of the experiment was to determine the sensitivity of the measure output to the orientation of the image, which will relate to issues concerning the digitisation of the image relative to a grid.

The results for spacing of the femur and tibia were obtained, and a sample results is presented as figure 5.

RESULTS

The alignment angles found for the X-ray images, using four threshold values of MSE and averaged over the other experimental conditions described in the section on

experiments, above, are shown in Table 1. The alignment angles found are similar and their variance is low, indicating rotational robustness of this technique. The experiments show the unwanted effect that the alignment angle found is dependent on image rotation. Table 2 is presented to show that both backtracking and no backtracking methods provide results equally sensitive to image rotation. The alignment angles found vary from 169.4° to 171.9° with backtracking and from 169.6° to 171.8° without backtracking. Both methods produce an average of 171.1° with a variance of 0.2°. The variation due to image rotation is small but present.

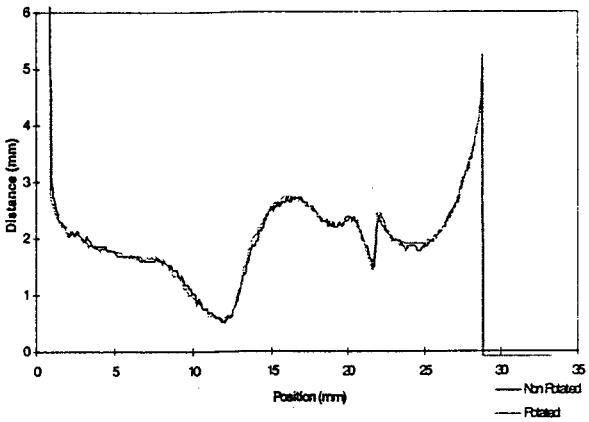

Figure 5. The distance measure plot obtained using this algorithm applied to the sample image used in this project. This plot incudes the effect of image rotation, which is considerably 'rougher' than the non-rotated image. He roughness results from quantisation effects in the rotation process.

The plot of the measurement of the distance between the femur and tibia in the image used is shown in figure 5. This figure shows a U-shaped trend, with the interesting features for clinical use shown in the detail of variations in the low spacing region.

CONCLUSIONS

The variance of angle of centreline intersection results from image quantisation effects. Although this is larger than desired, the measure of spacing will be affected only minimally, through a minor change in the slope of the line bisecting the intersection of the two bone centrelines, BL. Backtracking reduces the variance of the position of the centreline intersection point but the alignment angle shows no significant change. Thus backtracking makes little difference to the measure of distance obtained, although, given the improved consistency of the intersection angle, does lead to a marginal improvement in the distance measure quality.

ACKNOWLEDGMENTS

The author received the help of Michiel Janssen, a visiting student from University of Twente, The Netherlands, in

Table 1. The alignment angles found for various MSE thresholds, with and without backtracking.

MSE	Angle	σ_n
0.5	170.7	0.9
1	171.2	0.7
2	171.2	0.7
3	171.1	0.6
4	171.1	0.6
Av	171.1	0.8

a) With backtracking

MSE	Angle	σ_n
0.5	172.0	0.6
1	171.2	0.6
2	171.0	0.8
3	171.0	0.7
4	171.1	0.7
Av	171.1	0.7

b) Without backtracking

Table 2. The alignment angles as a function of image rotation.

Rotation	Angle	σ_n	Rotation	Angle	σ_n
25	170.5	0.4	25	169.4	0.5
20	171.3	0.2	20	170.5	0.2
15	171.3	0.1	15	170.7	0.2
10	171.3	0.2	10	170.9	0.1
5	171.7	0.2	5	171.6	0.2
0	171.8	0.2	0	171.7	0.2
-5	171.6	0.2	-5	171.9	0.1
-10	171.2	0.1	-10	171.7	0.03
-15	170.9	0.3	-15	171.7	0.2
-20	170.5	0.3	-20	170.9	0.3
-25	169.6	0.3	-25	170.6	0.3
Av	171.1	0.2	Av	171.1	0.2
a) Without backtracking			b) With backtracking		

writing the code to perform these tasks using Visual C++.

REFERENCES

[1] Stewein, J.C., Ferris, T.L.J., (1998), The asterisk operator – An edge detection operator addressing the problem of clean edges in bone X-ray images, *1998 Second International Conference on Knowledge-Based Intelligent Electronic Systems*, Adelaide, 21-23 April, vol 3, pp 28-31.

[2] M.A. Sid-Ahmed, Image Processing Theory, Algorithms, and Architectures, McGraw Hill, New York, 1994.

[3] R.C. Hardie, C.G. Boncelet, LUM filters: A class of rank-order-based filters for smoothing and sharpening, *IEEE Trans. SP*, **41**, 1061-1077, 1993.

[4] R.C. Hardie, C.G. Boncelet, Gradient-based edge detection using nonlinear edge enhancing prefilters, *IEEE Trans. IP*, **4**, 1572-1577, 1995.